



Absolute photoneutron cross sections of Sm isotopes

I. Gheorghe, H. Utsunomiya, D. Filipescu, T. Glodariu, H.-T. Nyhus, T. Renstro/m, O. Tesileanu, T. Shima, K. Takahisa, and S. Miyamoto

Citation: [AIP Conference Proceedings](#) **1645**, 327 (2015); doi: 10.1063/1.4909595

View online: <http://dx.doi.org/10.1063/1.4909595>

View Table of Contents: <http://scitation.aip.org/content/aip/proceeding/aipcp/1645?ver=pdfcov>

Published by the [AIP Publishing](#)

Articles you may be interested in

[PHOTONEUTRON CROSS SECTIONS FOR Au](#)

AIP Conf. Proc. **1377**, 362 (2011); 10.1063/1.3628413

[Threshold photoneutron cross sections for 208,207,206 Pb isotopes](#)

AIP Conf. Proc. **1238**, 231 (2010); 10.1063/1.3455937

[Enhanced photoneutron cross sections for zirconium isotopes near threshold: evidence for extra M1 strength?](#)

AIP Conf. Proc. **1012**, 173 (2008); 10.1063/1.2939288

[Photoneutron Cross Sections of Astrophysical Significance](#)

AIP Conf. Proc. **891**, 329 (2007); 10.1063/1.2713534

[Absolute photoionization cross section for C +](#)

AIP Conf. Proc. **500**, 218 (2000); 10.1063/1.1302655

Absolute photoneutron cross sections of Sm isotopes

I. Gheorghe ^{*}, H. Utsunomiya [†], D. Filipescu ^{**,*}, T. Glodariu ^{*}, H.-T. Nyhus [‡], T. Renstrøm [‡], O. Tesileanu ^{**}, T. Shima [§], K. Takahisa [§] and S. Miyamoto [¶]

^{*}National Institute for Physics and Nuclear Engineering Horia Hulubei, str. Atomistilor nr. 407, Romania

[†]Department of Physics, Konan University, Okamoto 8-9-1, Higashinada, Kobe 658-8501, Japan

^{**}Extreme Light Infrastructure - Nuclear Physics, str. Atomistilor nr. 407, Bucharest-Magurele, P.O.BOX MG6, Romania

[‡]Department of Physics, University of Oslo, N-0316 Oslo, Norway

[§]Research Center for Nuclear Physics, Osaka University, Suita, Osaka 567-0047, Japan

[¶]Laboratory of Advanced Science and Technology for Industry, University of Hyogo, 3-1-2 Kouto, Kamigori, Hyogo 678-1205, Japan

Abstract.

Photoneutron cross sections for seven samarium isotopes, ^{144}Sm , ^{147}Sm , ^{148}Sm , ^{149}Sm , ^{150}Sm , ^{152}Sm and ^{154}Sm , have been investigated near neutron emission threshold using quasimonochromatic laser-Compton scattering γ -rays produced at the synchrotron radiation facility NewSUBARU. The results are important for nuclear astrophysics calculations and also for probing γ -ray strength functions in the vicinity of neutron threshold. Here we describe the neutron detection system and we discuss the related data analysis and the necessary method improvements for adapting the current experimental method to the working parameters of the future Gamma Beam System of Extreme Light Infrastructure - Nuclear Physics facility.

INTRODUCTION

The Extreme Light Infrastructure - Nuclear Physics (ELI-NP) [1] is a large scale facility currently under development dedicated to nuclear physics with extreme electromagnetic fields. Two 10 PW lasers and one very brilliant Gamma Beam System (GBS) will be installed at ELI-NP. A very high intensity electric field of 10^{15} V/m spectral power and 10^{23} - 10^{23} W/cm² irradiance will be created at the interaction point of the two high power lasers synchronised in time and space.

Highly polarized (> 99%) tunable γ -ray beams of spectral density of 10^4 photons/s/eV will be produced by incoherent Compton back scattering of a laser beam off a very brilliant, intense, classical electron beam provided by a warm linac. Using green light lasers and electrons with tunable energies up to 720 MeV the GBS will provide γ -ray beams in the energy range from 200 keV to 19.5 MeV with a bandwidth better than 0.3% [2, 3].

The high intensity and very good energy resolution parameters of the polarized photon beam at ELI-NP will provide an excellent tool for investigating nuclear collective excitation modes. We plan to study the excitation and particle and gamma decay of Giant Resonances, mainly the Giant Dipole Resonance, pygmy dipole resonance and spin-flip M1 resonance.

The research team involved in conceiving the ELI-NP Technical Design Reports (TDR) has initiated an experimental campaign at the GACKO beam line of the synchrotron radiation facility NewSUBARU [4, 5], where photoneutron measurements in the vicinity of the neutron emission threshold (S_n) were performed on seven stable Sm isotopes. At NewSUBARU, γ -ray beams are produced by Compton scattering of photons delivered by top table industrial Nd:YVO₄ and CO₂ lasers from electrons with energies between 0.5 and 1.5 GeV stored in the NewSUBARU ring. The collimated γ -ray beam has a typical energy resolution of ~ 3 to 5 % and $\sim 10^5$ photons/second intensities.

Radiative neutron capture cross sections for ^{153}Sm (half-life: 1.928 d) and ^{151}Sm (half-life: 90 yr) were determined with the γ SF method [6, 7] using the present investigation of photoneutron cross sections on the Sm isotopes. The experimental procedure, data analysis and the theoretical analysis for the photoneutron emission and neutron capture cross sections are presented in [8].

We plan to develop a 4π high efficiency neutron detection setup for photoneutron cross sections measurements at ELI-NP. We will improve and adapt to the ELI-NP expected parameters the neutron detection system currently used at NewSUBARU. Here we discuss this neutron detection setup, the efficiency calibration and the related future

developments.

4 π NEUTRON DETECTION SETUP CURRENTLY IN USE AT NEWSUBARU

Fast neutrons with maximum energies up to approximately 7 MeV are emitted in (γ,n) reactions. A high efficiency 4 π triple-ring detector was used for recording the reaction neutrons and background neutrons. The background component was subtracted from the reaction plus background neutrons using the 100 Hz frequency pulsed time structure of the incident LCS γ -ray beam. For every 100 ms, reaction and background neutrons were recorded for 80 ms of irradiation and background neutrons only were recorded for 20 ms of beam-off.

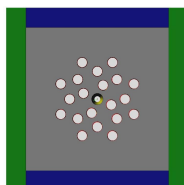


FIGURE 1. Schematics of fast neutron detector. 20 ^3He proportional counters are placed in three concentric rings. The inner ring is referred to as Ring 1, the middle ring as Ring 2 and the outer ring as Ring 3.

The neutron detection system was comprised of 20 cylindrical proportional counters, each containing 10 bars of ^3He , embedded in a neutron moderator, with the target placed at the center of the moderator. The neutron moderator was a $36 \times 36 \times 50 \text{ cm}^3$ block of polyethylene covered by additional 5 cm thick polyethylene plates with 1 mm thick cadmium metal for background neutron suppression. The proportional counters were placed equally spaced in three concentric rings, Ring 1, Ring 2 and Ring 3 of 4, 8 and respectively 8 proportional counters. A schematic image of the neutron detector is displayed in Figure 1.

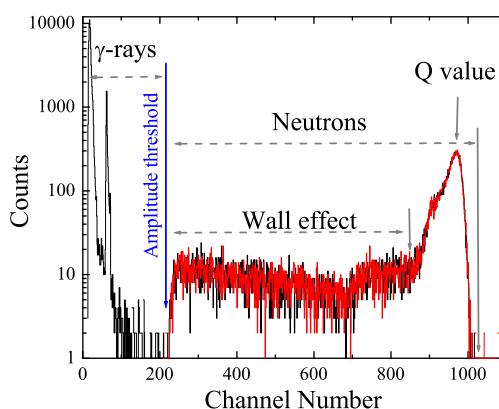


FIGURE 2. Energy spectra of a ^3He proportional counter obtained with a ^{252}Cf source placed in the center of the polyethylene moderator. The neutron and γ induced counts are discriminated by a simple amplitude threshold.

The gas ^3He is widely used as a detection medium for neutrons for the reaction: $^3\text{He} + n \rightarrow ^4\text{He}^* \rightarrow ^3\text{H} + p$. For reactions induced by slow neutrons, the Q values of 764 keV leads to opposite directed reaction products with energies: $E_p = 0.573 \text{ MeV}$ and $E_{^3\text{H}} = 0.191 \text{ MeV}$. The thermal neutron cross section for this reaction is 5330 barns, significantly higher than that other elements used for neutron counters, such as boron, and its value also falls off with a $1/v$ energy dependence, where v is the neutron velocity.

Figure 2 shows a typical energy spectra of a ^3He proportional counter. The energy peak corresponds to the Q value of the reaction, namely the events when both of the reaction products are stopped in the ^3He gas. At lower energies we have a wide flat energy range for the events when either the tritium or the proton is stopped in the detector's wall, energy area called the *wall effect* plateau.

Gamma induced counts are clearly separated by the charged particle induced counts, as their amplitude is much lower. Therefore the gamma - neutron discrimination can be easily performed by applying an amplitude threshold. Figure 2 shows the raw spectra, with no threshold, in black line and the neutron spectra, in red line. The threshold level is applied just below the *wall effect* plateau.

Energy calibration

The triple ring neutron detector with ^3He proportional counters is designed to achieve a high total efficiency of detecting neutrons in the energy range below 1 MeV with a capability of deducing the average neutron energy by the so called *ring ratio* technique.

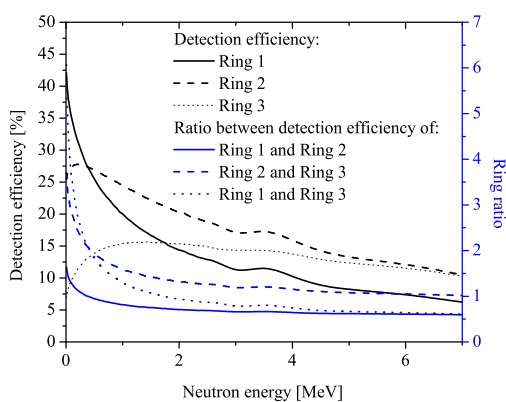


FIGURE 3. Neutron detection efficiency of each of the counter rings. Ratio between the efficiency on ring and another.

The *ring ratio* technique, which is used for determining the average energy for a given sample target nuclide as a function of the incident γ -ray beam average energy, was originally developed by Berman et al. [9]. Because the amount of moderator material between the neutron emission point and each ring of detectors is different, different rings of detectors have different detection efficiencies for neutrons of equal energy.

Figure 3 shows results of an MCNP Monte Carlo simulation of the efficiencies of Ring1, Ring2 and Ring3 as a function of neutron energy. As can be seen in Figure 3, the Ring 1 is more sensitive to low energy neutrons than the other two rings and less sensitive to fast neutrons, as there is little moderating material between it and the irradiated target. The situation for Ring 3 is reversed, having a low efficiency for slow and high efficiency for fast neutrons, due to large amount of moderating material between it and the target.

As can be seen in Figure 3, the ratio of the number of neutrons detected in one ring to that in another ring is sensitive to the average neutron energy. Using this energy dependency we can determine the average neutron energy for a given target nucleus for each γ -ray beam energy and the neutron detection efficiency.

Ring ratio data

The ring ratio data for ^{144}Sm , ^{147}Sm , ^{148}Sm , ^{149}Sm , ^{150}Sm , ^{152}Sm and ^{154}Sm are presented in Figures 4 through 7, respectively. The photoneutron process in the samarium isotopes is generally characterized by a rise of the average neutron energy in the energy range above the (γ, n) threshold (S_n) up to 13 MeV, the maximum photon energy investigated in this study. The maximum value of the average neutron energy is of about 1 MeV for all the investigated nuclei.

The ^{144}Sm data have a distinct behaviour, as the average neutron energy has a slow rise up to 11.75 MeV and then decreases with higher photon energy values, as shown in Figure 4. The ^{144}Sm target had a 88.8 % enrichment, the remaining 11.2 % were represented by the other samarium isotopes. As ^{144}Sm has the neutron emission value higher than all the other isotopes, a significant part of the reaction neutrons recorded during irradiation were emitted in (γ, n) reactions on $^{147,148,149,150,152,154}\text{Sm}$. The average neutron energy for these reactions at approximately 11 MeV incident photon energy is ~ 1 MeV. The maximum energy of the neutrons emitted in the $^{144}\text{Sm}(\gamma, n)^{143}\text{Sm}$ for the incident photon energy $E_\gamma = 10.659$ MeV is $E_{max}^n = (A - 1) \cdot (E_\gamma - S_n) / A$ of 0.138 MeV, where A is the mass number. Therefore the average neutron energy determined using the *ring ratio* method for ^{144}Sm in the vicinity of S_n is biased due the presence of impurity nuclei inside the target, which produce reaction neutrons with energies considerably higher than of the ones produced by reactions on ^{144}Sm .

For the two even - odd nuclei investigated in the present study, ^{147}Sm and ^{149}Sm , the *ring ratio* data are much more scattered than for the even - even nuclei, as shown in Figures 5, while ^{148}Sm , ^{150}Sm , ^{152}Sm and ^{154}Sm exhibit a smooth dependence with incident photon energy. For ^{148}Sm the average neutron energy rises sharply to an asymptotic value

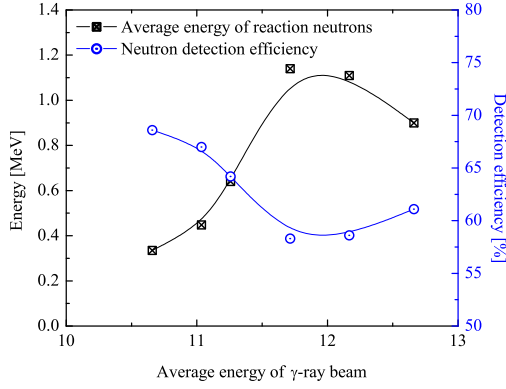


FIGURE 4. Average energy of neutrons from $^{144}\text{Sm}(\gamma,n)^{143}\text{Sm}$ reaction obtained with the *ring ratio* technique and the corresponding neutron detection efficiency as a function of incident LCS γ -ray beam average energy expressed in MeV.

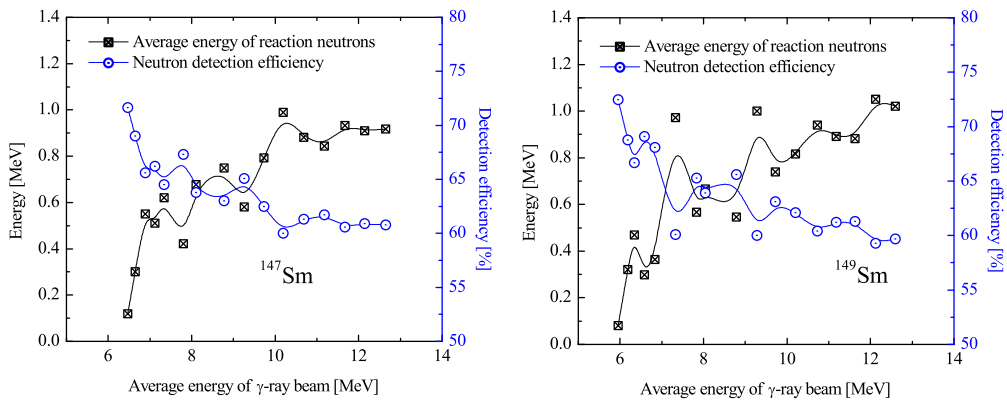


FIGURE 5. Same as Figure 4 but for $^{147}\text{Sm}(\gamma,n)^{146}\text{Sm}$ (left image) and $^{149}\text{Sm}(\gamma,n)^{148}\text{Sm}$ (right image).

of ~ 0.9 MeV, with a possible structure effect below 9 MeV as shown in Figure 6 (left). ^{150}Sm , ^{152}Sm and ^{154}Sm have a slower rise of the neutron average energy above the S_n , with possible structure effects at 8.5, 9.5 and 11.2 MeV for ^{150}Sm , at 8.4 MeV for ^{152}Sm and at 9.7 and 10.7 MeV for ^{154}Sm , as shown in Figures 6 (right) and 7.

If the energy difference between the incident photon energy and the neutron emission threshold of the target nucleus is below the first excited state in the residual nucleus, the neutron energy is determined using $E^n = (A - 1) \cdot (E_\gamma - S_n) / A$. This is the case for the first three data points in ^{147}Sm and ^{149}Sm , the first two points in ^{150}Sm and the first point in ^{148}Sm .

CONCLUSIONS AND FUTURE WORK

Photoneutron cross section measurements above the neutron emission threshold have been performed for all seven stable samarium isotopes. The neutron detection efficiency values for each of the sample target and each incident photon beam average energy have been determined using the *ring ratio* method developed by [9] and described above.

We intend to further develop the method in order to apply it to future experiments at the ELI-NP facility. The *ring ratio* method does not take into consideration the reaction neutron energy spectra, but only the average neutron energy. But the reaction neutron energy spectra are considerably different from one nucleus to another, especially in the vicinity of the neutron emission threshold. We plan to simulate the response of a neutron detector to a neutron evaporation spectra obtained from Hauser Feshbach statistical model calculations performed with the code EMPIRE [10]. Thus we will investigate the neutron detection efficiency dependence with neutron evaporation spectra and also with angular anisotropy of reaction neutrons. Using Geant4 simulations, we also plan to develop a flat efficiency neutron detector. The response of such a detector is not affected by the shape of the neutron evaporation spectra.

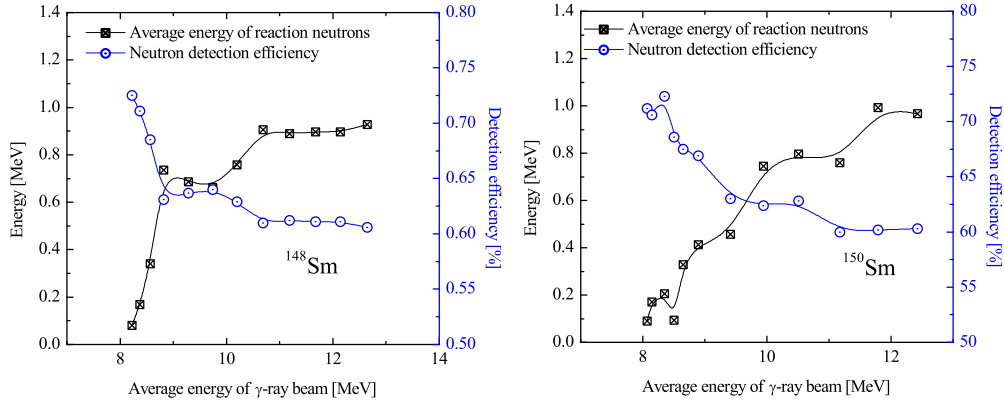


FIGURE 6. Same as Figure 4 but for $^{148}\text{Sm}(\gamma,n)^{147}\text{Sm}$ (left image) and $^{150}\text{Sm}(\gamma,n)^{149}\text{Sm}$ (right image).

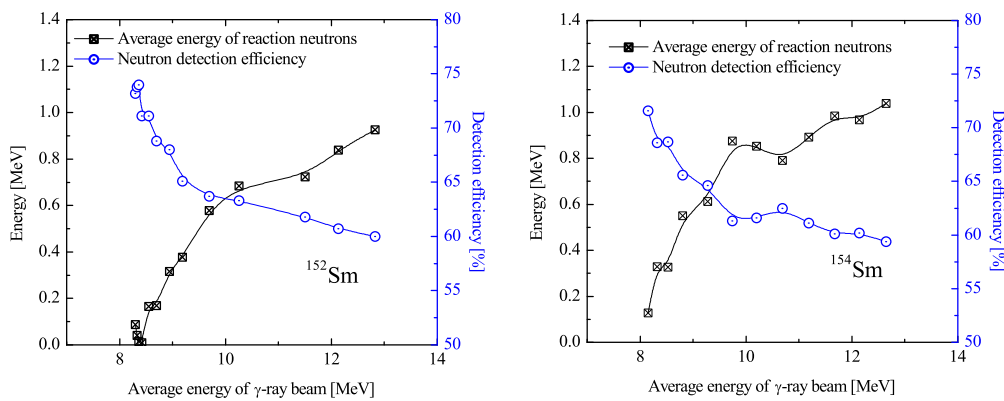


FIGURE 7. Same as Figure 4 but for $^{152}\text{Sm}(\gamma,n)^{151}\text{Sm}$ (left image) and $^{154}\text{Sm}(\gamma,n)^{153}\text{Sm}$ (right image).

Another important issue to be treated is the development of neutron detection systems using BF_3 and ^{10}B neutron counters, as ^3He is not commercially available nowadays.

ACKNOWLEDGMENTS

D. Filipescu and O. Tesileanu acknowledge financial support from the Extreme Light Infrastructure Nuclear Physics (ELI-NP) Phase I, a project co-financed by the European Union through the European Regional Development Fund.

REFERENCES

1. N. Zamfir, *EPJ Web of Conf.* **66**, 11043 (2014).
2. C. Vaccarezza, *IPAC 2012 Conference, in Proc. p. TUOBB01* (2012).
3. V. Petrillo, *NIM A* **693**, 109 (2012).
4. S. Amano, *NIM A* **602**, 337–341 (2009).
5. K. Horikawa, *NIM A* **618**, 209–215 (2010).
6. H. Utsunomiya, *Phys. Rev C* **80**, 055806 (2009).
7. H. Utsunomiya, *Phys. Rev C* **82**, 064610 (2010).
8. D. Filipescu, *Submitted to Phys. Rev. C* (2014).
9. B. L. Berman, *Rev. Mod. Phys.* **47**, 713–761 (1975).
10. M. Herman, *Nucl. Data Sheets* **108**, 2655 (2007).